Probing nanomagnetism with quantum sensors: from antiferromagnets to 2D materials

Aurore Finco

Laboratoire Charles Coulomb
Team Solid-State Quantum Technologies (S2QT)

CNRS and Université de Montpellier, Montpellier, France

Rice-Europe Workshop on spintronics, May 23th 2023

slides available at https://magimag.eu

How can we use a quantum system to probe nanomagnetism?

How can we use a quantum system to probe nanomagnetism?

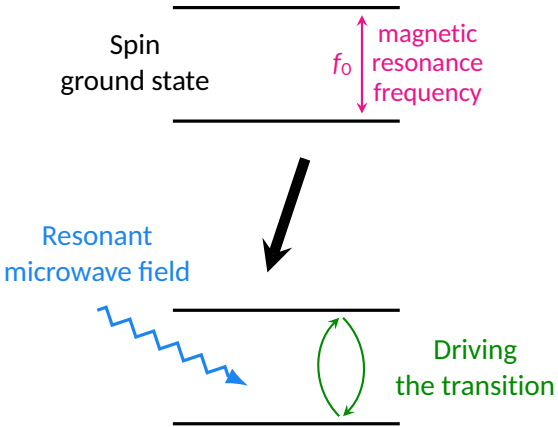

How can we use a quantum system to probe nanomagnetism?

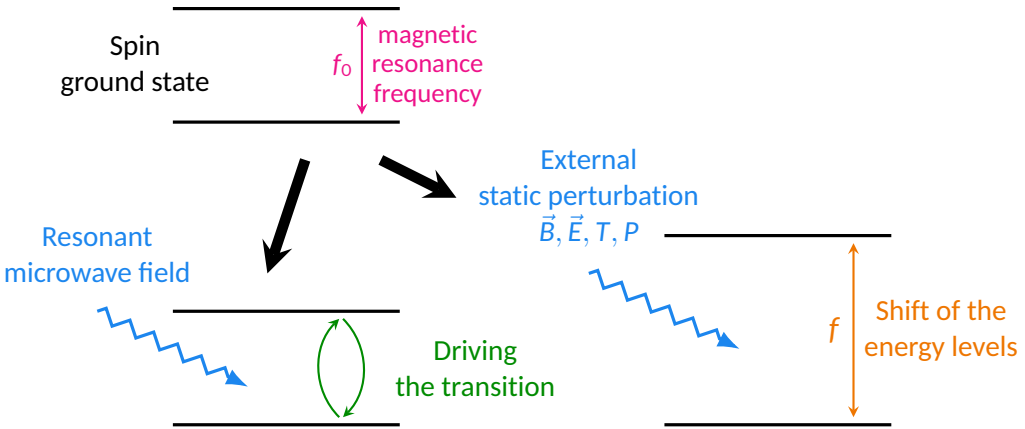

How can we use a quantum system to probe nanomagnetism?

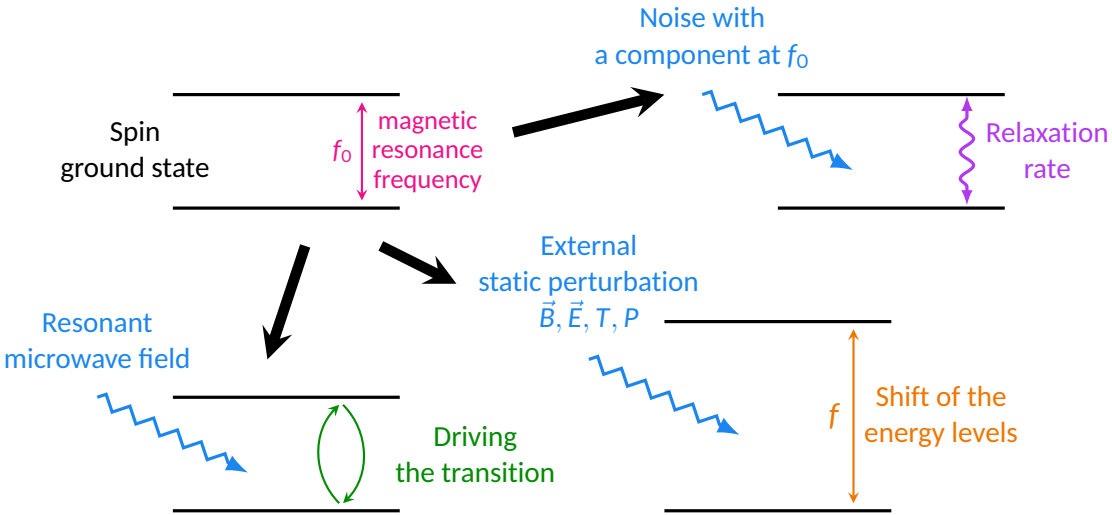

How can we use a quantum system to probe nanomagnetism?

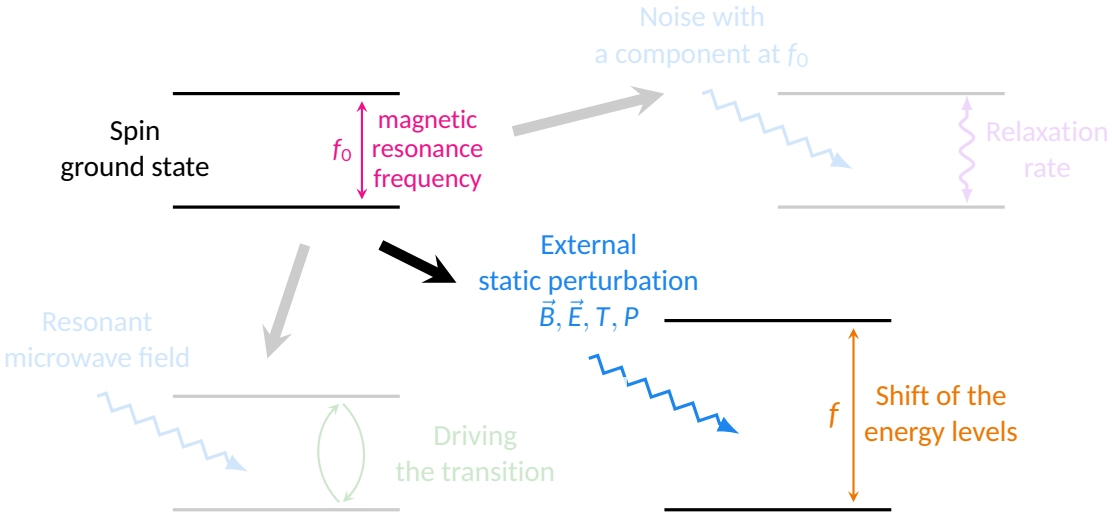

Outline

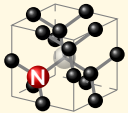

Scanning NV center microscopy

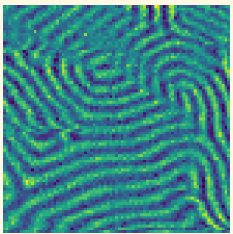

Imaging of complex
antiferromagnetic textures

Outline

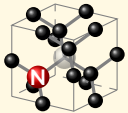

Scanning NV center microscopy

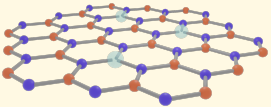

Sensing with V_B^- in h-BN

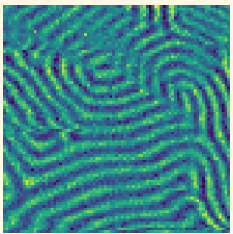

Imaging of complex
antiferromagnetic textures

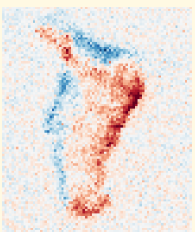

Investigation of
van der Waals magnets

NV centers as magnetic field sensors

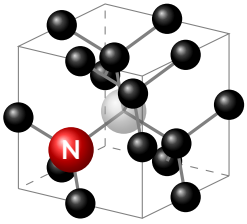

Nitrogen-Vacancy defect
in diamond

NV centers as magnetic field sensors

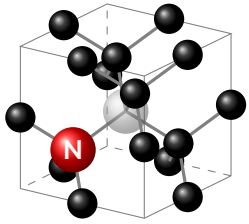

Nitrogen-Vacancy defect
in diamond

- Optical manipulation and reading
- Ambient conditions

NV centers as magnetic field sensors

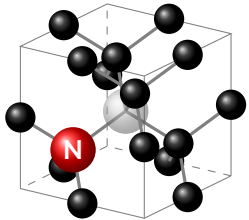

Nitrogen-Vacancy defect
in diamond

- Optical manipulation and reading
- Ambient conditions

Spin-dependent fluorescence

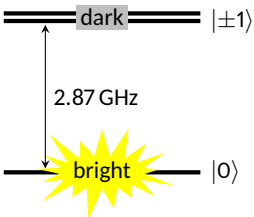

NV ground state
spin $S = 1$

NV centers as magnetic field sensors

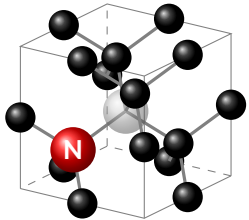

Nitrogen-Vacancy defect
in diamond

- Optical manipulation and reading
- Ambient conditions

Spin-dependent fluorescence

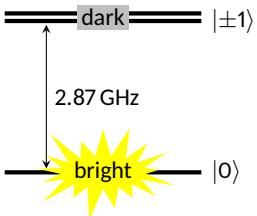

NV ground state
spin $S = 1$

green laser
excitation
NV polarized
in $|0\rangle$

NV centers as magnetic field sensors

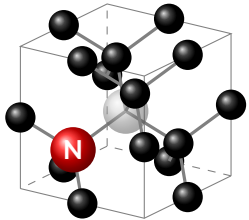

Nitrogen-Vacancy defect
in diamond

- Optical manipulation and reading
- Ambient conditions

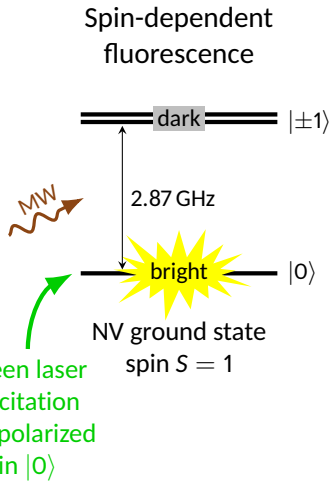

NV centers as magnetic field sensors

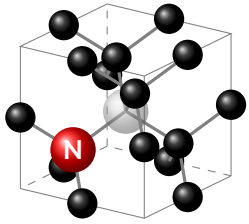

Nitrogen-Vacancy defect in diamond

- Optical manipulation and reading
- Ambient conditions

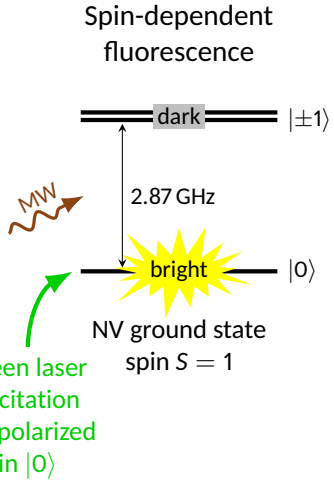

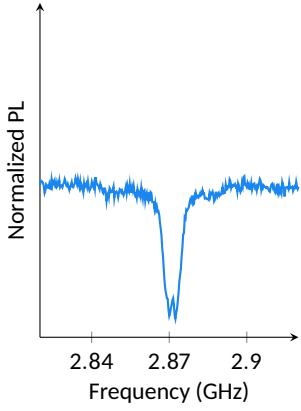

NV centers as magnetic field sensors

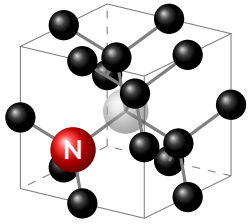

Nitrogen-Vacancy defect in diamond

- Optical manipulation and reading
- Ambient conditions

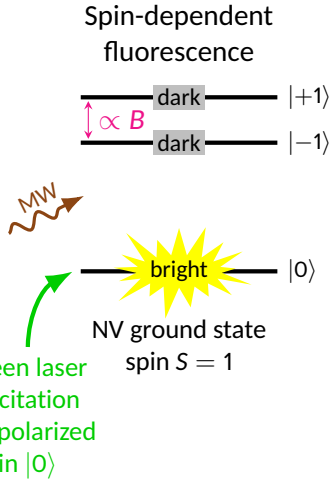

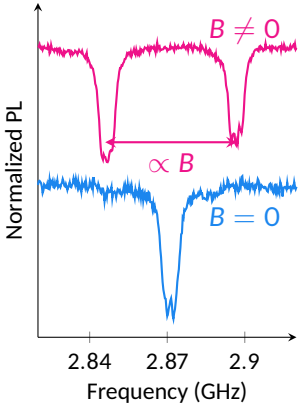

NV centers as magnetic field sensors

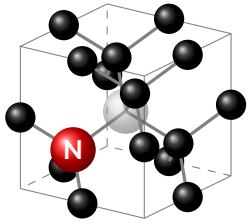

Nitrogen-Vacancy defect in diamond

- Optical manipulation and reading
- Ambient conditions

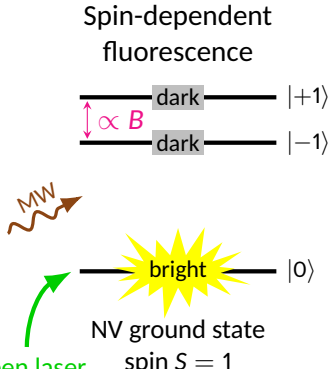

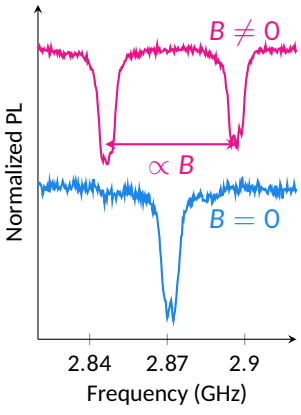

Sensitivity: a few $\mu T/\sqrt{Hz}$

Scanning NV center microscopy

Diamond
AFM tip

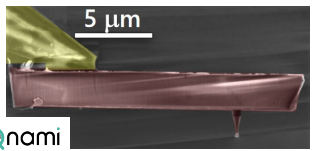

Qnami

P. Maletinsky *et al.* *Nat. Nano.* 7 (2012), 320

Scanning NV center microscopy

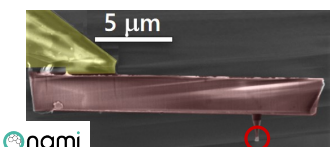

Implanted single
NV center

P. Maletinsky *et al.* *Nat. Nano.* 7 (2012), 320

Scanning NV center microscopy

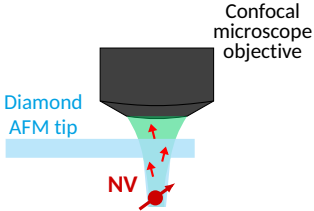

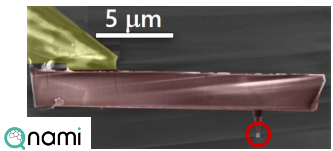

Implanted single
NV center

P. Maletinsky *et al.* *Nat. Nano.* 7 (2012), 320

Scanning NV center microscopy

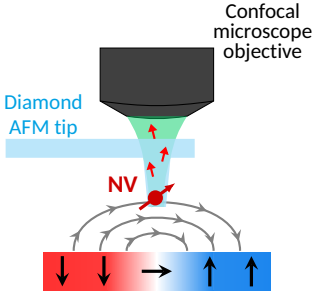

Implanted single
NV center

P. Maletinsky *et al.* *Nat. Nano.* 7 (2012), 320

Scanning NV center microscopy

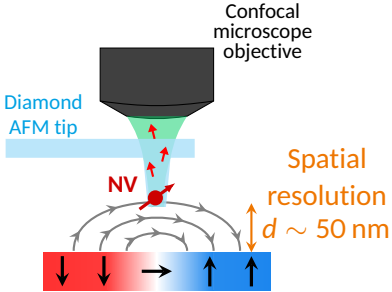

P. Maletinsky *et al.* *Nat. Nano.* 7 (2012), 320

Scanning NV center microscopy

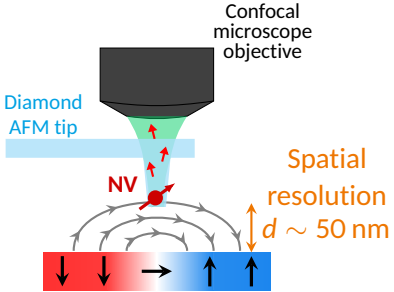

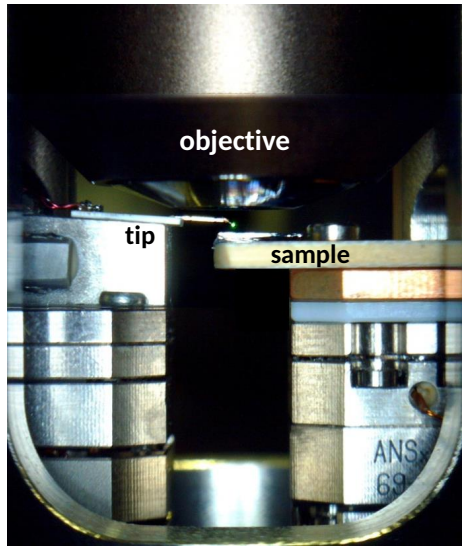

P. Maletinsky *et al.* *Nat. Nano.* 7 (2012), 320

Bismuth ferrite, a room-temperature multiferroic

Electric polarization

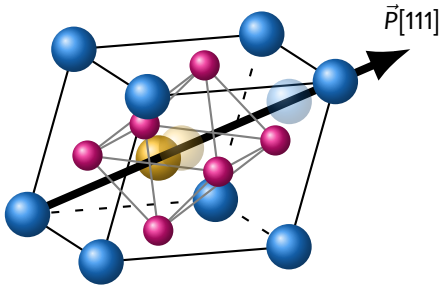

Ferroelectric phase (T<1100 K)

G. Catalan *et al.* *Adv. Mater.* 21 (2009), 2463–2485

Bismuth ferrite, a room-temperature multiferroic

Electric polarization

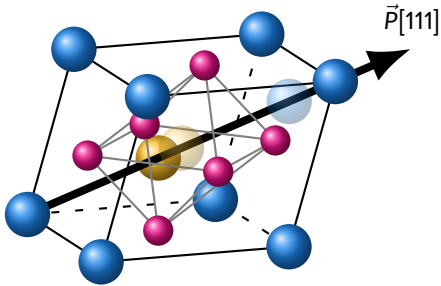

Ferroelectric phase (T<1100 K)

Magnetism

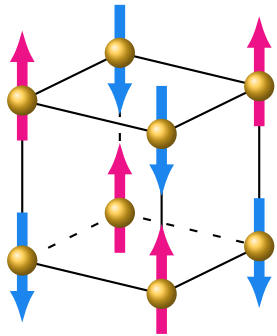

G-type antiferromagnetic phase ($T_N = 643$ K)

G. Catalan *et al.* *Adv. Mater.* 21 (2009), 2463–2485

The effects of magnetoelectric coupling in $BiFeO_3$

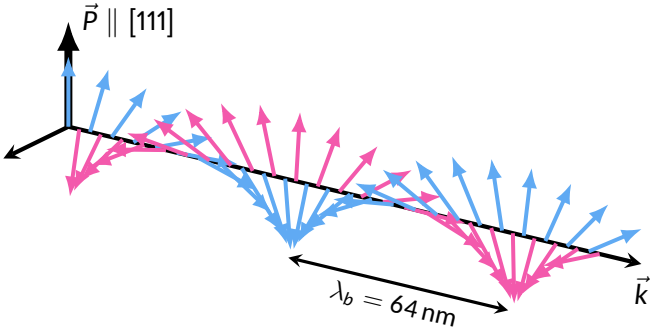

Fully compensated cycloid

$\rightarrow$ **No stray field!**

The effects of magnetoelectric coupling in $BiFeO_3$

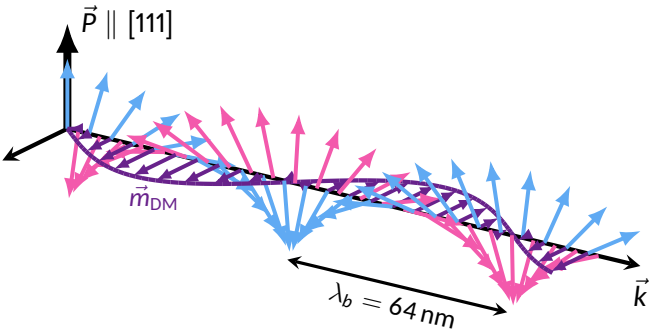

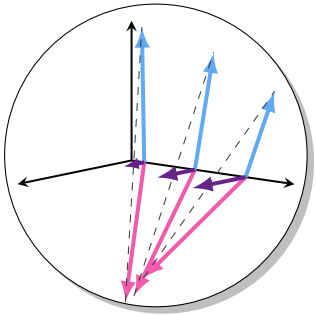

Spin density wave
Weak uncompensated moment
$\rightarrow$ **Small stray field**

M. Ramazanoglu *et al*. *Phys. Rev. Lett.* 107 (2011), 207206

The effects of magnetoelectric coupling in $BiFeO_3$

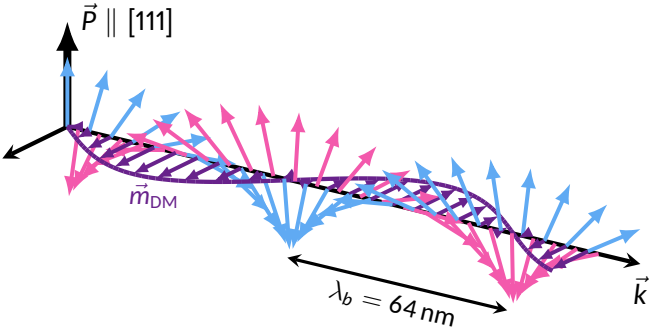

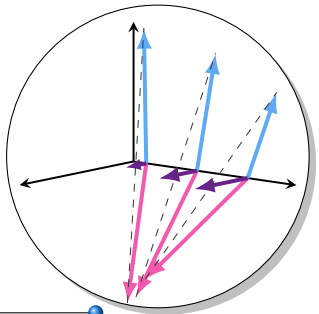

Spin density wave
Weak uncompensated moment
$\rightarrow$ **Small stray field**

M. Ramazanoglu *et al.* *Phys. Rev. Lett.* 107 (2011), 207206

The cycloid in a low strained $BiFeO_3$ thin film

Collaborations: UMR CNRS/Thales, Palaiseau (V. Garcia, S. Fusil)
CEA SPEC, Gif-sur-Yvette (J.-Y. Chauleau, M. Viret)

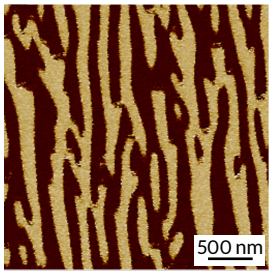

PFM image
ferroelectric domains

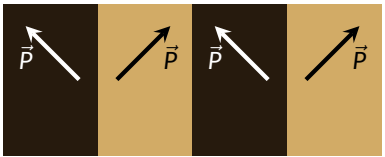

I. Gross *et al*. *Nature* 549 (2017), 252–256

The cycloid in a low strained $BiFeO_3$ thin film

Collaborations: UMR CNRS/Thales, Palaiseau (V. Garcia, S. Fusil)
CEA SPEC, Gif-sur-Yvette (J.-Y. Chauleau, M. Viret)

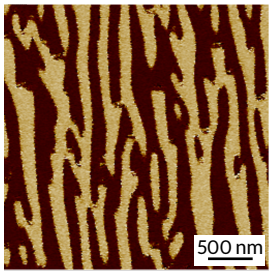

PFM image
ferroelectric domains

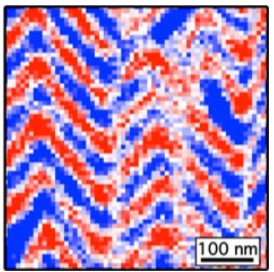

NV image
cycloid

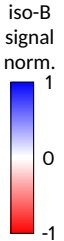

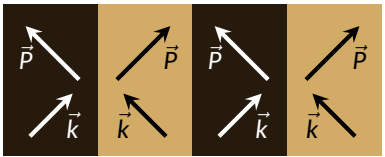

I. Gross *et al*. *Nature* 549 (2017), 252–256

The cycloid in a low strained $BiFeO_3$ thin film

Collaborations: UMR CNRS/Thales, Palaiseau (V. Garcia, S. Fusil)
CEA SPEC, Gif-sur-Yvette (J.-Y. Chauleau, M. Viret)

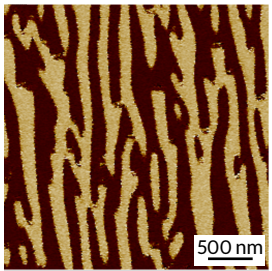

PFM image
ferroelectric domains

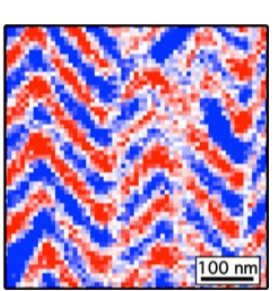

NV image
cycloid

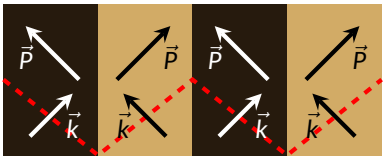

I. Gross *et al*. *Nature* 549 (2017), 252–256

Quantitative analysis of the cycloid in bulk single crystal

Collaborations: UMR CNRS/Thales, Palaiseau (V. Garcia, S. Fusil)
CEA SPEC, Gif-sur-Yvette (J.-Y. Chauleau, M. Viret)

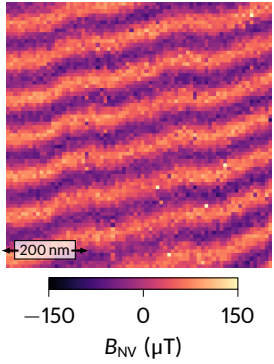

Quantitative analysis of the cycloid in bulk single crystal

Collaborations: UMR CNRS/Thales, Palaiseau (V. Garcia, S. Fusil)
CEA SPEC, Gif-sur-Yvette (J.-Y. Chauleau, M. Viret)

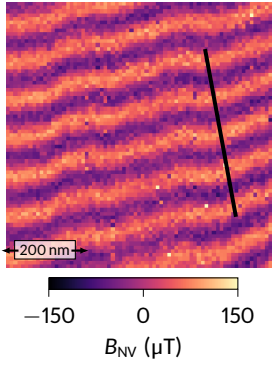

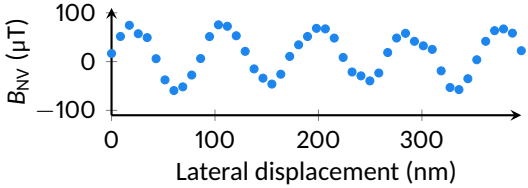

Quantitative analysis of the cycloid in bulk single crystal

Collaborations: UMR CNRS/Thales, Palaiseau (V. Garcia, S. Fusil)
CEA SPEC, Gif-sur-Yvette (J.-Y. Chauleau, M. Viret)

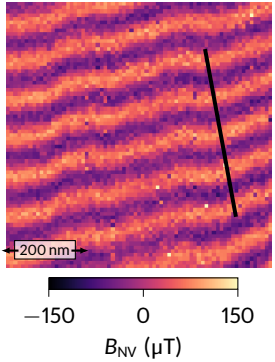

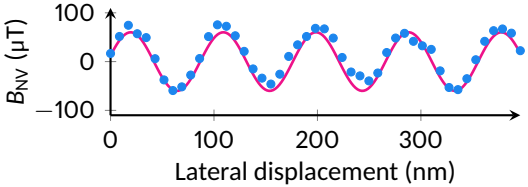

$$\begin{cases} B_x = 0 \\ B_y = -\dfrac{A}{\sqrt{2}}\left(\mathrm{Re}\{S\} - \mathrm{Im}\{S\}\right) \\ B_z = \sqrt{2}\,A\,\mathrm{Re}\{S\} \end{cases} \quad \text{with} \quad \begin{cases} \mathrm{A} = \dfrac{\mu_0 m_{\mathrm{DM}}}{\sqrt{3}\,a^3}\sinh\left(\dfrac{ka}{2\sqrt{2}}\right) \\ \mathrm{S} = e^{-kz/\sqrt{2}} e^{ik(y-z)/\sqrt{2}} \dfrac{1-e^{-kt(1+i)/\sqrt{2}}}{1-e^{-ka(1+i)/\sqrt{2}}} \end{cases}$$

Quantitative analysis of the cycloid in bulk single crystal

Collaborations: UMR CNRS/Thales, Palaiseau (V. Garcia, S. Fusil)
CEA SPEC, Gif-sur-Yvette (J.-Y. Chauleau, M. Viret)

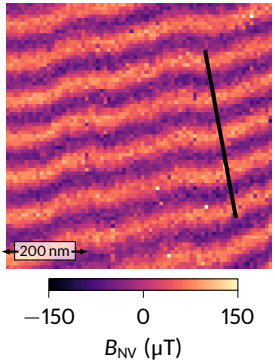

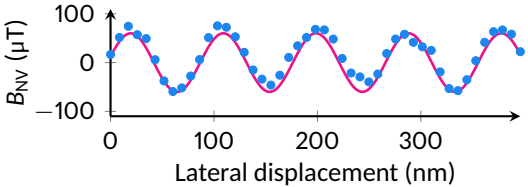

$$m_{DM} = 0.09 \pm 0.03\ \mu_B$$

M. Ramazanoglu *et al.* *Phys. Rev. Lett.* 107 (2011), 207206

$$\begin{cases} B_x = 0 \\ B_y = -\dfrac{A}{\sqrt{2}}\left(\mathrm{Re}\{S\} - \mathrm{Im}\{S\}\right) \\ B_z = \sqrt{2}\,A\,\mathrm{Re}\{S\} \end{cases} \quad \text{with} \quad \begin{cases} A = \dfrac{\mu_0 m_{DM}}{\sqrt{3}\,a^3}\sinh\left(\dfrac{ka}{2\sqrt{2}}\right) \\ S = e^{-kz/\sqrt{2}} e^{ik(y-z)/\sqrt{2}}\,\dfrac{1-e^{-kt(1+i)/\sqrt{2}}}{1-e^{-ka(1+i)/\sqrt{2}}} \end{cases}$$

Rotation of the cycloid propagation direction measured in real space...

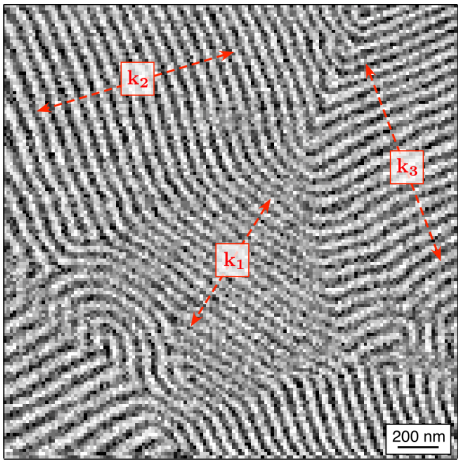

Rotation of the cycloid propagation direction measured in real space...

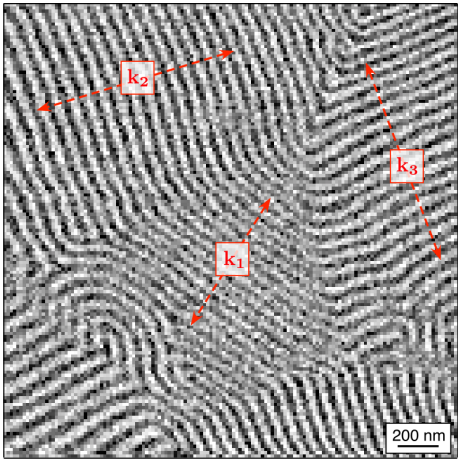

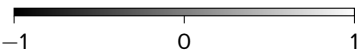

iso-B signal

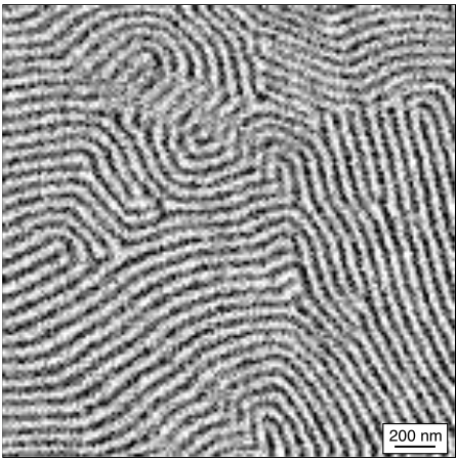

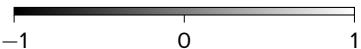

iso-B signal

… and in reciprocal space

Resonant X-ray scattering

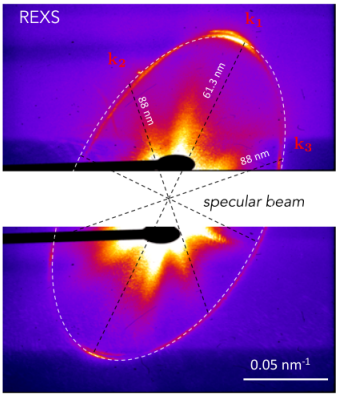

SOLEIL SYNCHROTRON

N. Jaouen

… and in reciprocal space

Resonant X-ray scattering

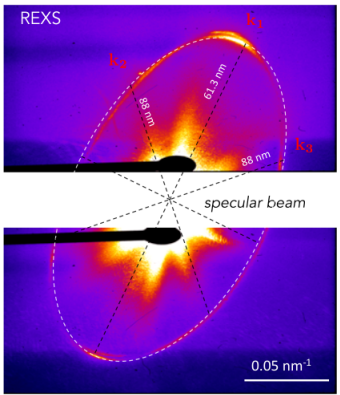

Polar plot of $\frac{2\pi}{\lambda}$ vs $\vec{k}$ direction

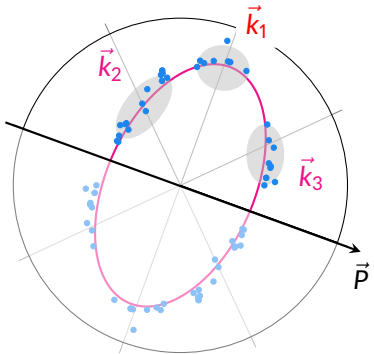

SOLEIL SYNCHROTRON

N. Jaouen

… and in reciprocal space

Resonant X-ray scattering

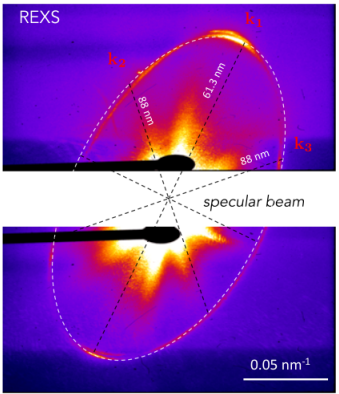

Polar plot of $\frac{2\pi}{\lambda}$ vs $\vec{k}$ direction

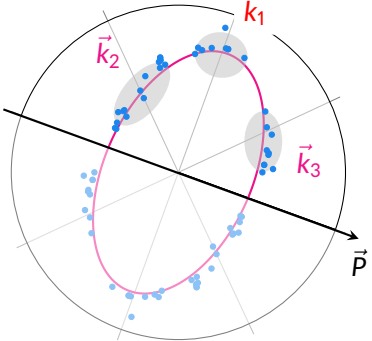

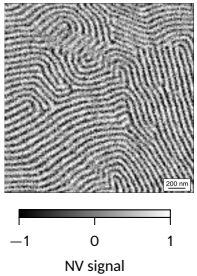

SOLEIL SYNCHROTRON

N. Jaouen

… and in reciprocal space

Resonant X-ray scattering

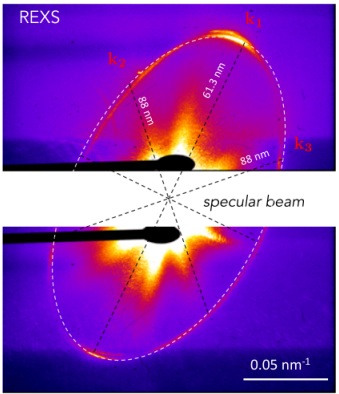

Polar plot of $\frac{2\pi}{\lambda}$ vs $\vec{k}$ direction

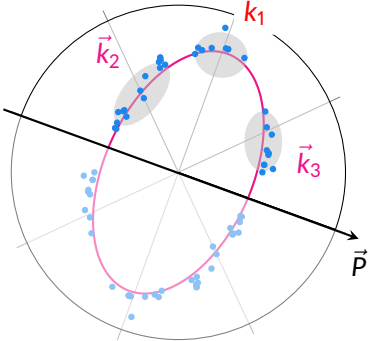

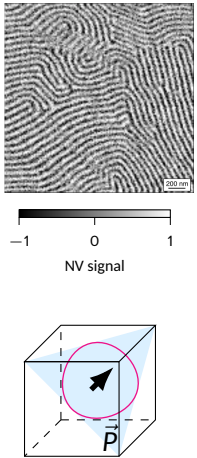

SOLEIL SYNCHROTRON

N. Jaouen

… and in reciprocal space

Resonant X-ray scattering

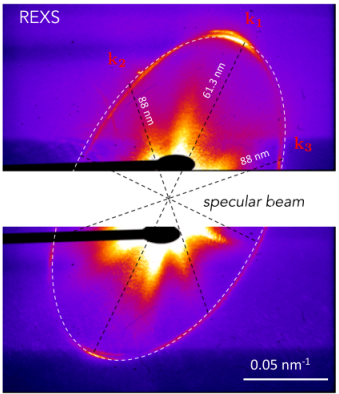

Polar plot of $\frac{2\pi}{\lambda}$ vs $\vec{k}$ direction

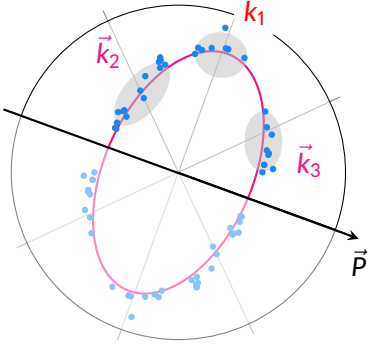

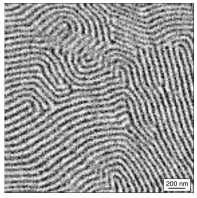

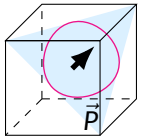

Surface effect? Only $\vec{k}_1$ seen by neutrons

D. Lebeugle *et al.* *Phys. Rev. Lett.* 100 (2008), 227602

SOLEIL SYNCHROTRON

N. Jaouen

Universal patterns in lamellar systems

Block copolymer
Period 40 nm

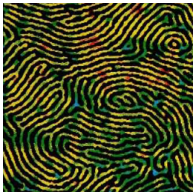

T. A. Witten. *Phys. Today* 43 (1990), 21

$BiFeO_3$ magnetic cycloid
Period 64 nm

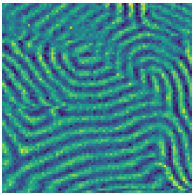

A. Finco *et al.* *Phys. Rev. Lett.* 128 (2022), 187201

FeGe magnetic helix
Period 70 nm

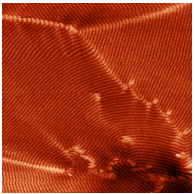

P. Schönherr *et al.* *Nat. Phys.* 14 (2018), 465

Liquid crystals
Period 800 nm

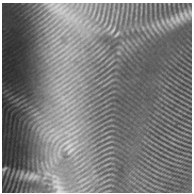

Y. Bouligand. *Dislocations in solids* (1983), Chap. 23

Ferrimagnetic garnet
Period 8 µm

M. Seul *et al.* *Phys. Rev. A* 46 (1992), 7519

Fluid diffusion
Period 250 µm

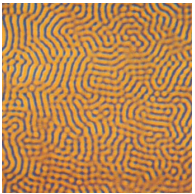

Q. Ouyang *et al.* *Chaos* 1 (1991), 411

Topological defects in $BiFeO_3$

$+\pi$-disclination

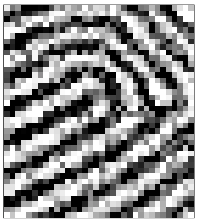

$-\pi$-disclination

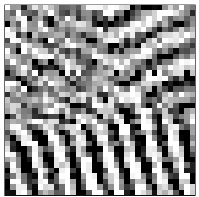

Edge dislocation

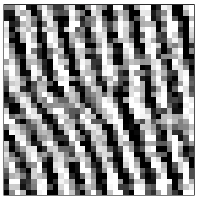

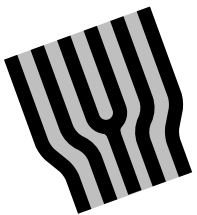

Perspective: electrical control?

Outline

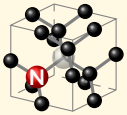

Scanning NV center microscopy

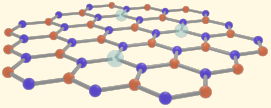

Sensing with V_B^- in h-BN

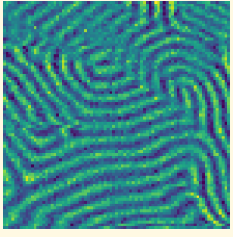

Imaging of complex
antiferromagnetic textures

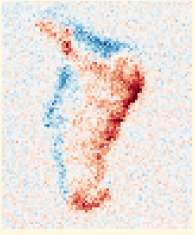

Investigation of
van der Waals magnets

Imaging magnetic van der Waals materials

Collaboration: Institut Néel, Grenoble (A. Purbawati, J. Coraux, N. Rougemaille)

Scanning NV center magnetometry on $CrTe_2$
2D ferromagnet at room temperature
with in-plane magnetization

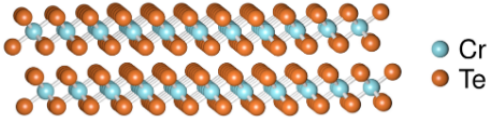

F. Fabre *et al.* *Phys. Rev. Mater.* 5 (2021), 034008

Imaging magnetic van der Waals materials

Collaboration: Institut Néel, Grenoble (A. Purbawati, J. Coraux, N. Rougemaille)

Scanning NV center magnetometry on $CrTe_2$
2D ferromagnet at room temperature
with in-plane magnetization

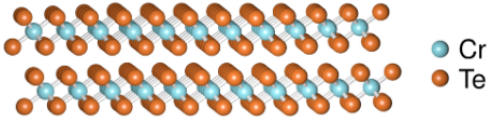

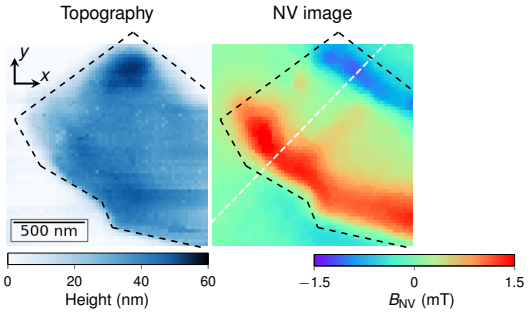

F. Fabre *et al.* *Phys. Rev. Mater.* 5 (2021), 034008

Imaging magnetic van der Waals materials

Collaboration: Institut Néel, Grenoble (A. Purbawati, J. Coraux, N. Rougemaille)

Scanning NV center magnetometry on $CrTe_2$
2D ferromagnet at room temperature
with in-plane magnetization

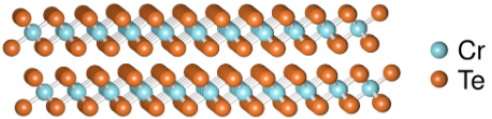

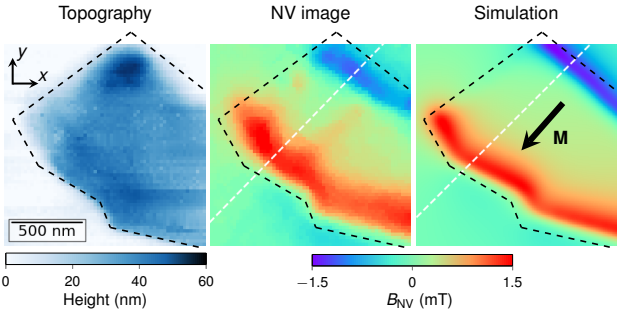

F. Fabre *et al.* *Phys. Rev. Mater.* 5 (2021), 034008

Imaging magnetic van der Waals materials

Collaboration: Institut Néel, Grenoble (A. Purbawati, J. Coraux, N. Rougemaille)

Scanning NV center magnetometry on $CrTe_2$
2D ferromagnet at room temperature
with in-plane magnetization

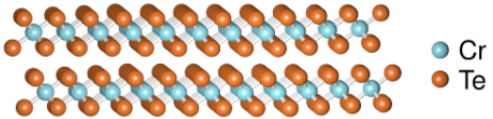

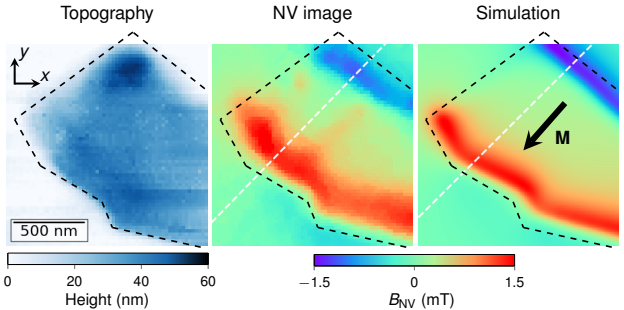

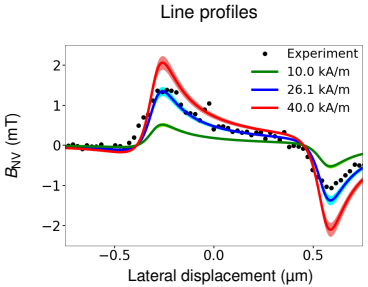

$CrTe_2$ is not stable in air $\rightarrow$ encapsulation with h-BN

F. Fabre *et al.* *Phys. Rev. Mater.* 5 (2021), 034008

Defects in h-BN

- h-BN is a wide bandgap material (about 6 eV)
- Single photon emitters were known in h-BN

T. T. Tran *et al*. *Nature Nanotechnology* 11 (2016), 37

Defects in h-BN

- h-BN is a wide bandgap material (about 6 eV)
- Single photon emitters were known in h-BN

T. T. Tran *et al*. *Nature Nanotechnology* 11 (2016), 37

- A **spin defect** was identified in 2020

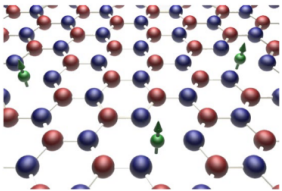

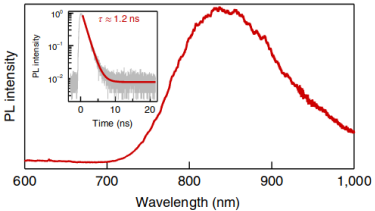

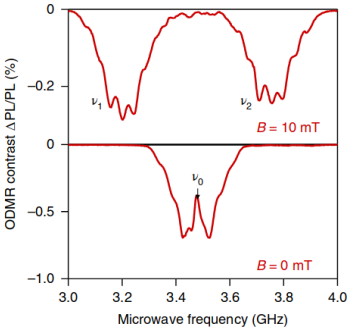

A. Gottscholl *et al*. *Nat. Mater.* 19 (2020), 540

Objective: a quantum sensing foil integrated in the van der Waals heterostructure

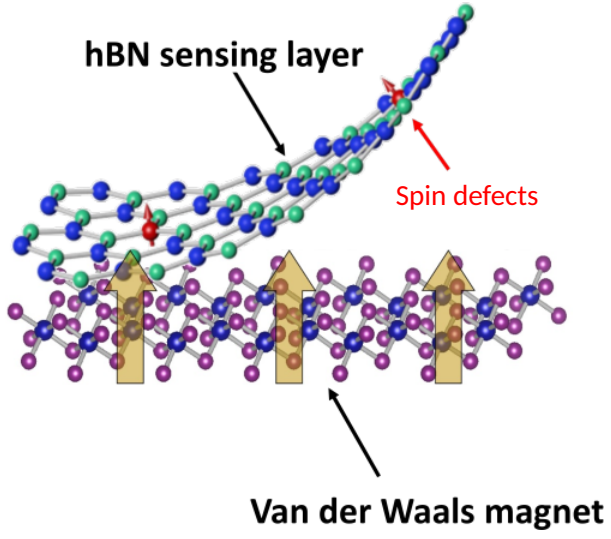

Creating ensembles of boron vacancies in h-BN

Collaboration: Kansas State University (J. Li, J. Edgar)

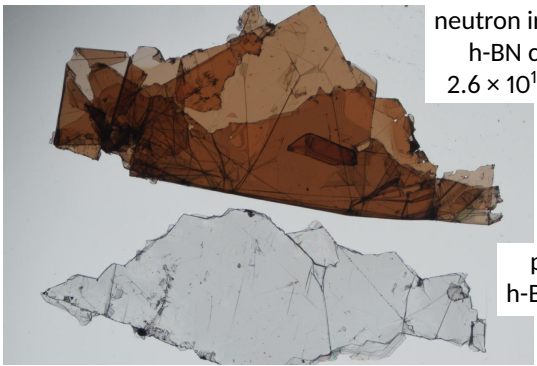

S. Liu *et al.* *Chem. of Mater.* 30 (2018), 6222

Creating ensembles of boron vacancies in h-BN

Collaboration: Kansas State University (J. Li, J. Edgar)

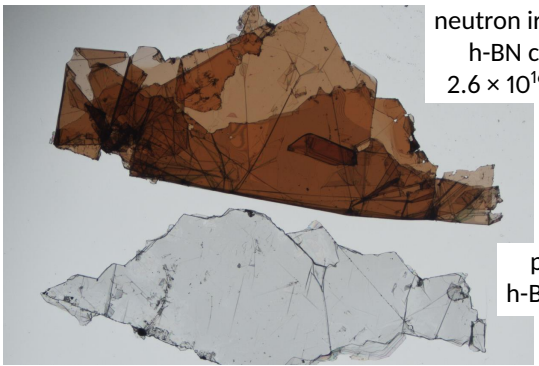

S. Liu *et al.* *Chem. of Mater.* 30 (2018), 6222

- Excitation at 532 nm
- Ambient conditions

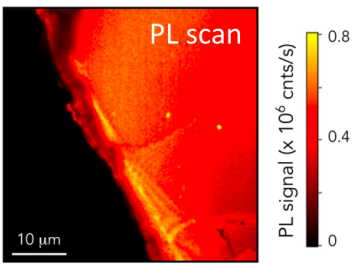

A. Haykal *et al.* *Nat. Commun.* 13 (2022), 4347

Measuring magnetic fields with V_B^-

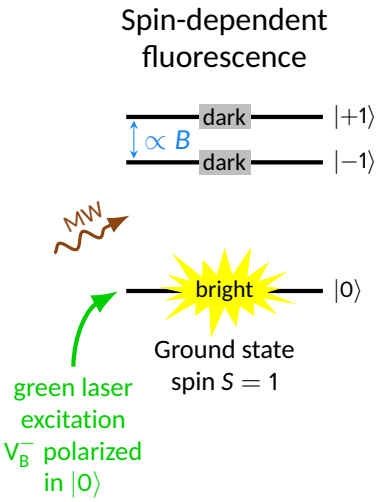

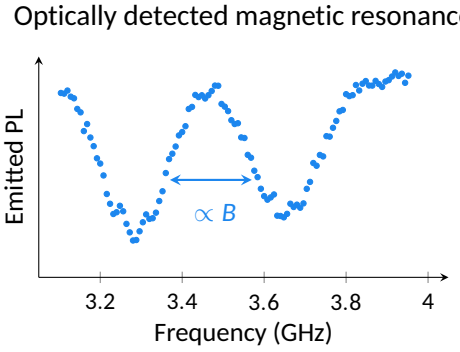

Magnetic field sensitivity

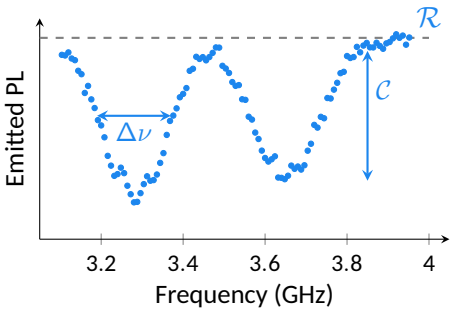

$$\eta \sim 0.7 \, \frac{1}{\gamma_e} \, \frac{\Delta\nu}{\mathcal{C}\sqrt{\mathcal{R}}}$$

P. Kumar *et al.* *Phys. Rev. Appl.* 18 (2022), L061002

Magnetic field sensitivity

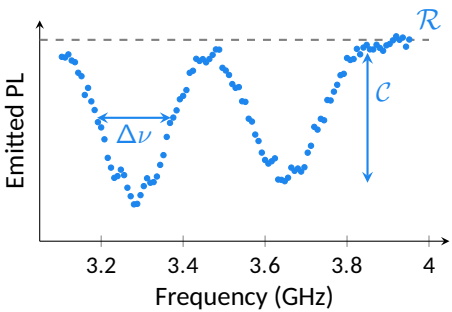

$$\eta \sim 0.7 \, \frac{1}{\gamma_e} \, \frac{\Delta\nu}{\mathcal{C}\sqrt{\mathcal{R}}}$$

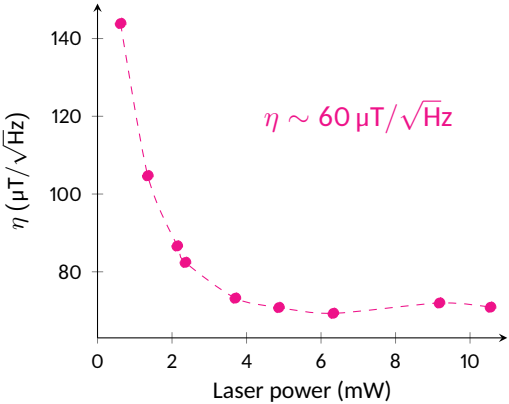

P. Kumar *et al.* *Phys. Rev. Appl.* 18 (2022), L061002

Imaging a $CrTe_2$ flake

Collaboration: Institut Néel, Grenoble and LPCNO, Toulouse

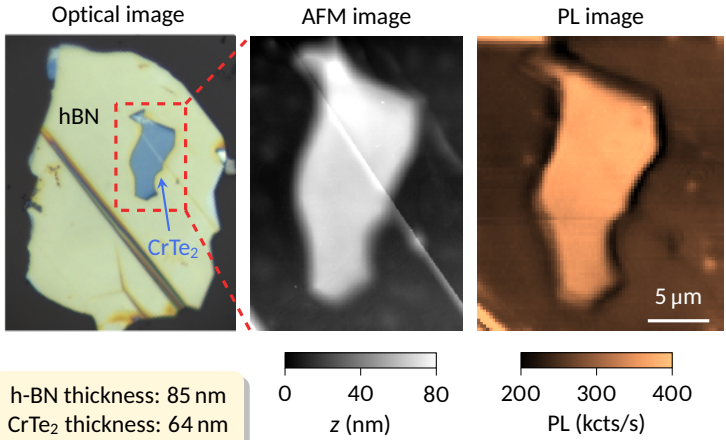

h-BN thickness: 85 nm
$CrTe_2$ thickness: 64 nm

P. Kumar *et al.* *Phys. Rev. Appl.* 18 (2022), L061002

Imaging a $CrTe_2$ flake

Collaboration: Institut Néel, Grenoble and LPCNO, Toulouse

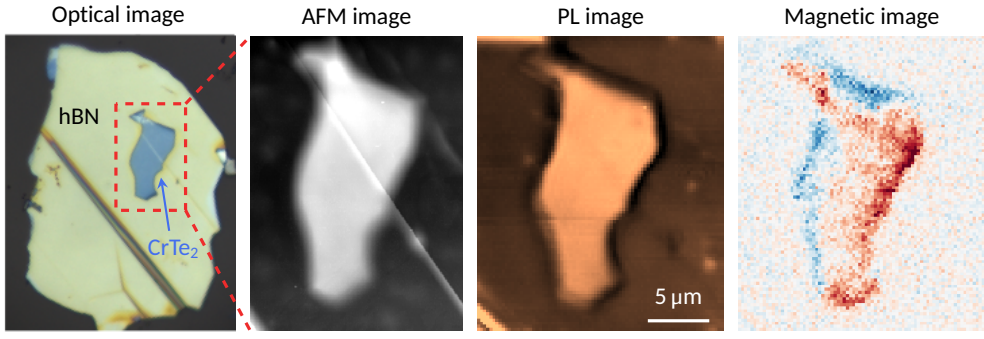

h-BN thickness: 85 nm
$CrTe_2$ thickness: 64 nm

P. Kumar *et al.* *Phys. Rev. Appl.* 18 (2022), L061002

Comparison with simulations

Two averaging procedures are necessary:

- Vertically, over the h-BN film thickness
- Laterally, over the gaussian profile of the laser beam

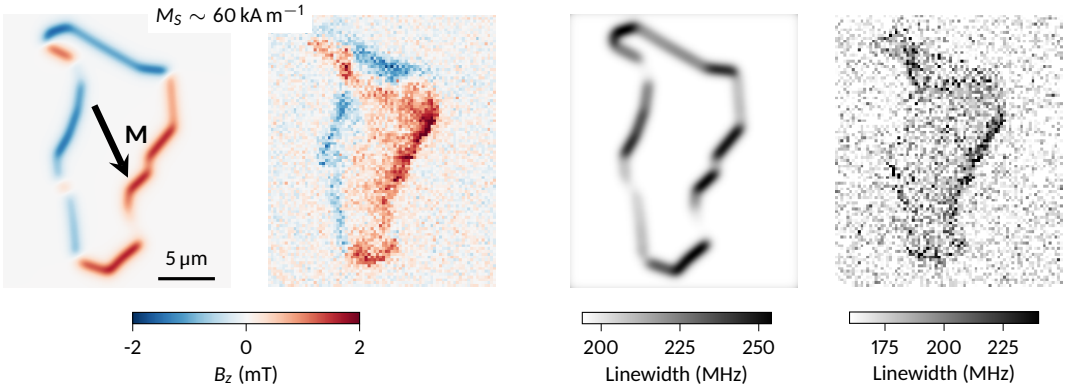

$\rightarrow$ **Being really quantitative is difficult, using thinner flakes would help!**

Using thinner flakes

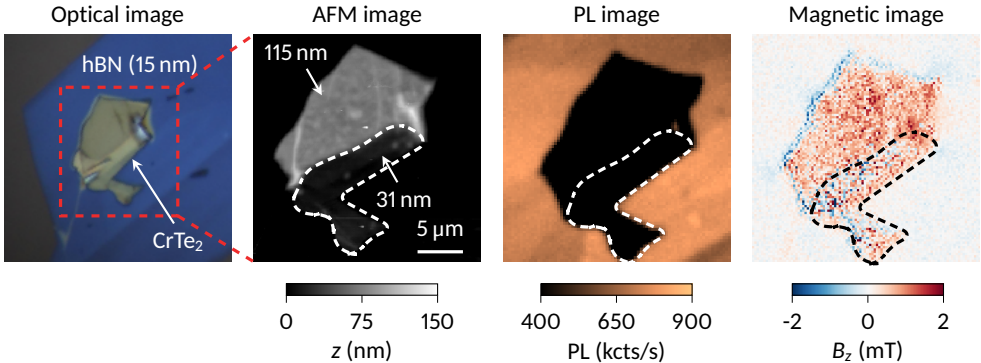

- PL quenching effect at the metallic surface of $CrTe_2$
- Need for larger laser excitation power
- Heating of the magnetic material, crossing T_C

Summary

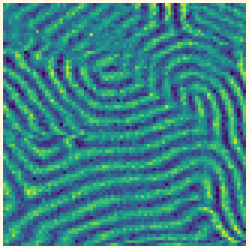

Imaging topological defects
in a multiferroic antiferromagnet
with NV centers

A. Finco *et al.* *Phys. Rev. Lett.* 128 (2022), 187201

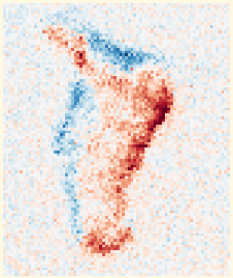

Imaging 2D magnets
with defects in h-BN

P. Kumar *et al.* *Phys. Rev. Appl.* 18 (2022), L061002

Acknowledgments

L2C, Montpellier
Pawan Kumar, Florentin Fabre, Alrik Durand, Tristan Clua-Provost, Zhao Mu, Bernard Gil, Guillaume Cassabois, Isabelle Robert-Philip, Vincent Jacques

UMR CNRS/Thales, Palaiseau
Pauline Dufour, Vincent Garcia, Stéphane Fusil, Karim Bouzehouane

SPEC, CEA Gif-sur-Yvette
Anne Forget, Dorothée Colson, Jean-Yves Chauleau, Michel Viret

Synchrotron Soleil
Nicolas Jaouen

Kansas State University, USA
Jiahan Li, James Edgar

Institut Néel, Grenoble, France
Johann Coraux, Nicolas Rougemaille

LPCNO, Toulouse, France
Cédric Robert, Jules Fraunie, Pierre Renucci, Xavier Marie